Structure and spectroscopic properties of Er^{3+}/Ce^{3+} co-doped TeO_2-Bi_2O_3-TiO_2 glasses modified with various WO_3 contents for 1.53 μm emission*

ZHENG Shi-chao (郑世超)**, **QI Ya-wei** (齐亚伟), **PENG Sheng-xi** (彭胜喜), **YIN Dan-dan** (殷丹丹), **ZHOU Ya-xun** (周亚训), **and DAI Shi-xun** (戴世勋)

College of Information Science and Engineering, Ningbo University, Ningbo 315211, China

(Received 31 July 2013)

The Er^{3+}/Ce^{3+} co-doped tellurite-based glasses (TeO_2-Bi_2O_3-TiO_2) modified with various WO_3 contents are prepared using conventional melt-quenching technique. The X-ray diffraction (XRD) patterns and Raman spectra of glass samples are measured to investigate the structures. The absorption spectra, the up-conversion emission spectra, the 1.53 μm band fluorescence spectra and the lifetime of Er^{3+}:$^4I_{13/2}$ level are measured, and the amplification quality factors of Er^{3+} are calculated to evaluate the effect of WO_3 contents on the 1.53 μm band spectroscopic properties. With the introduction of WO_3, it is found that the prepared tellurite-based glasses maintain the amorphous structure, while the 1.53 μm band fluorescence intensity of Er^{3+} is improved evidently, and the fluorescence full width at half maximum (FWHM) is broadened accordingly. In addition, the prepared tellurite-based glass samples have larger bandwidth quality factor than silicate and germanate glasses. The results indicate that the prepared Er^{3+}/Ce^{3+} co-doped tellurite-based glass with a certain amount of WO_3 is an excellent gain medium applied for the 1.53 μm band Er^{3+}-doped fiber amplifier (EDFA).

Document code: A **Article ID:** 1673-1905(2013)06-0461-4

DOI 10.1007/s11801-013-3137-9

Tellurite-based glasses possess a variety of interesting and important optical and material properties, such as good transparency in the visible (VIS) and infrared regions (0.4—6 μm), high dielectric constant, high refractive index (~2), low melting temperature and good solubility for rare earth dopants (10 to 50 times larger than that in silica), and the properties in their potential applications have increased considerably over the last few years[1-6]. Indeed, many optical devices, including Er^{3+}-doped fiber amplifiers (EDFAs), lasers and planar waveguides, have been fabricated by the tellurite-based glasses[3,7].

Under the excitation of a commercial 980 nm laser diode (LD), a strong up-conversion emission resulting from the excited state absorption (ESA) of Er^{3+} at the pump level $^4I_{11/2}$ is observed in Er^{3+}-doped tellurite glasses applied for the 1.53 μm band EDFA[8], which is ascribed to the low phonon energy (~750 cm^{-1}) of glass hosts. The low phonon energy of tellurite glass restrains the rapid multi-phonon relaxation process of Er^{3+} from the pump level $^4I_{11/2}$ to the fluorescence emitting level $^4I_{13/2}$, and in turn results in a weakened 1.53 μm band fluorescence emission. In order to improve the 1.53 μm band fluorescence intensity, it is necessary to suppress the ESA of Er^{3+}, i.e., to decrease the lifetime of Er^{3+} at the pump level $^4I_{11/2}$ and then to increase the Er^{3+} populations at the fluorescence emitting level $^4I_{13/2}$. To this end, an effective Er^{3+}/Ce^{3+} co-doped scheme is adopted to provoke the non-radiative decay from the $^4I_{11/2}$ level to $^4I_{13/2}$ level through the energy transfer of Er^{3+}:$^4I_{11/2}$+Ce^{3+}:$^2F_{5/2}$→Er^{3+}:$^4I_{13/2}$+Ce^{3+}: $^2F_{7/2}$[9,10].

In this paper, a relatively large phonon energy oxide of WO_3 is introduced into the Er^{3+}/Ce^{3+} co-doped tellurite glass (TeO_2-Bi_2O_3-TiO_2) to further improve the 1.53 μm band fluorescence, since a large energy mismatch (~1200 –1400 cm^{-1}) exists between the transitions of Ce^{3+}:$^2F_{5/2}$ →$^2F_{7/2}$ and Er^{3+}:$^4I_{11/2}$→$^4I_{13/2}$[10,11].

The Er^{3+}/Ce^{3+} co-doped tellurite glasses with (78.75–x)-TeO_2-10Bi_2O_3-10TiO_2-$x$$WO_3-0.5Er_2O_3-0.75Ce_2O_3$ (x= 0%, 3%, 6%, 9% and 12%) were prepared in alumina crucibles at 1000–1100 ˚C for about 30 min. The obtained glass melts were annealed at about 330 ˚C for 120 min, then were cut and well polished for optical measurements. The obtained glass samples were denoted as TBW0–TBW4, respectively. For a comparison, the Er^{3+} single-doped tellurite glass sample with 79.5TeO_2-10Bi_2O_3-

* This work has been supported by the National Natural Science Foundation of China (No.61178063), the Graduate Innovative Scientific Research Project of Zhejiang Province (No.YK2010048), the Scientific Research Foundation of Graduate School of Ningbo University (No.G13035), and the K. C. Wong Magna Fund and Hu Lan Outstanding Doctoral Fund in Ningbo University.

** E-mail:526522025@qq.com

$10TiO_2$-$0.5Er_2O_3$ was prepared and denoted as TBT.

The Raman spectra were measured by Renishaw micro-Raman instrument. Powder X-ray diffraction (XRD) pattern was recorded using a power diffractometer of Bruker D2 with Cu Ka radiation (30 kV×10 mA). The absorption spectra were measured with a Lamda 950 UV/VIS/NIR spectrophotometer. The up-conversion and fluorescence emission spectra were recorded with a TRIAX550 spectrophotometer under the excitation of a 980 nm LD. The fluorescence lifetime of Er^{3+} was measured with light pulses of 980 nm LD and a TDS1012 100 MHz oscilloscope.

In order to analyze the amorphous structure of TBW0–TBW4 samples, powder XRD measurements were carried out, and the measured XRD patterns are presented in Fig.1. It can been seen that all glass samples possess nearly identical XRD patterns, and the introduction of WO_3 does not give rise to any intensive discrete or sharp diffraction peak, but broadens the humps, which is the characteristic of amorphous materials[12], indicating that the synthesized glass samples maintain the amorphous structure.

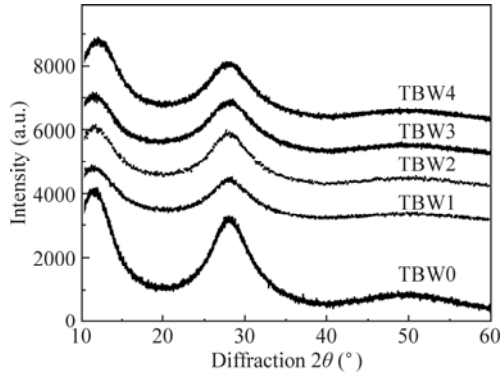

Fig.1 XRD patterns of the powder TBW0-TBW4 samples

Fig.2 displays the measured Raman spectra of TBW0 and TBW1 glass samples. The Raman scattering band centered around 420 cm^{-1} is assigned to the stretching vibration of Te-O-Te or O-Te-O linkages between two [TeO_4] four-coordinate atoms, and the bands centered around 660 cm^{-1} and 750 cm^{-1} originate from the stretching vibration of Te-O bond in the continuous networks composed of [TeO_4] trigonal bipyramid and [$TeO_{3+\delta}$] trigonal pyramid structural units, respectively. A new Raman scattering peak centered around 920 cm^{-1} is observed, which is attributed to the characteristic stretching vibration modes of W-O- or W=O bonds associated with the [WO_4] and [WO_6] structural units[13]. The results indicate that the maximum phonon energy of glass host increases from 750 cm^{-1} to about 920 cm^{-1} when introducing WO_3.

Fig.3 displays the measured absorption spectra of Er^{3+} single-doped TBT and Er^{3+}/Ce^{3+} co-doped TBW0–TBW4 samples in the wavelength range of 400–1700 nm. All absorption peaks are marked with different excited levels, and they originate from the transitions between the ground state, $^4I_{15/2}$ and various excited states of $^4I_{13/2}$, $^4I_{11/2}$, $^4I_{9/2}$, $^4F_{9/2}$, $^4S_{3/2}$, $^2H_{11/2}$, $^4F_{7/2}$ and $^4F_{5/2}$ of Er^{3+}, respectively[14]. Compared with that of Er^{3+} single-doped TBT sample, the absorption spectra of the Er^{3+}/Ce^{3+} co-doped TBW0–TBW4 samples shift from the UV-side absorption edge towards the longer wavelength direction because of the intensive inter-configurational transition of Ce^{3+}[15]. With the increase of WO_3 content, the absorption band shapes and their barycenters are found to be almost identical except for some differences in the band intensities, indicating that WO_3 component has no evident effect on the position distribution of the lowest Stark sub-levels.

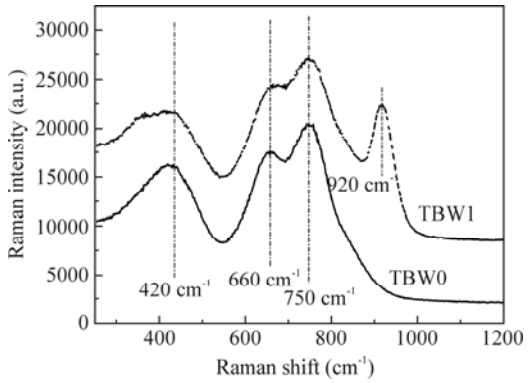

Fig.2 Raman spectra of TBW0 and TBW1 samples

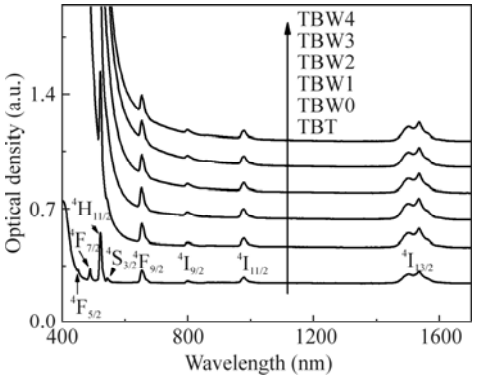

Fig.3 Absorption spectra of TBT and TBW0–TBW4 samples

Under the excitation of 980 nm LD, the measured up-conversion emission spectra of TBW0 sample in the wavelength range of 500–700 nm, along with the green and red up-conversion intensities changing with the WO_3 content, are presented in Fig.4. The up-conversion emission can be observed clearly in the TBW0 sample without WO_3, in which green up-conversion emissions centered around 526 nm and 547 nm are attributed to the $^2H_{11/2}\rightarrow{}^4I_{15/2}$ and $^4S_{3/2}\rightarrow{}^4I_{15/2}$ transitions, respectively, while the slightly weaker red up-conversion emission centered around 661 nm is ascribed to the $^4F_{9/2}\rightarrow{}^4I_{15/2}$ transition of Er^{3+}. The up-conversion mechanism and the relevant excited-state emitting levels ($^4S_{3/2}$, $^2H_{11/2}$ and

$^4F_{9/2}$) involved in the luminescence process are well explained in Fig.5. It can be found that both the green and red up-conversion emissions originate from the ESA of Er^{3+} at the $^4I_{11/2}$ level, and their up-conversion intensities decrease rapidly with the increase of WO_3 content. For the prepared TBW0–TBW4 samples with the same Er^{3+}/Ce^{3+} co-doped concentration, the decrease of up-conversion emission intensity with the increase of WO_3 content is obviously the enhanced result of the non-radiative decay process from the pump level $^4I_{11/2}$ to the fluorescence emitting level $^4I_{13/2}$ aroused by the enhanced energy transfer process between Er^{3+}/Ce^{3+} ions, which will be discussed later.

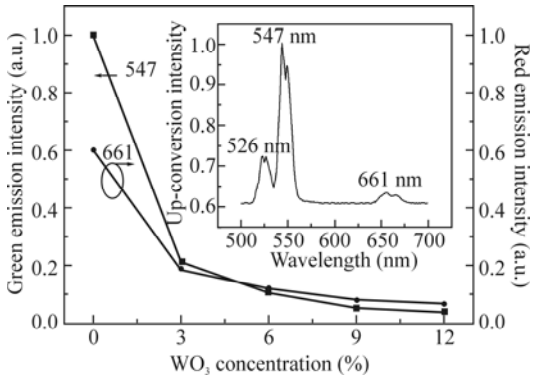

Fig.4 Green and red up-conversion emission intensities as a function of WO_3 content (The inset is up-conversion emission spectrum of TBW0 sample under the 980 nm excitation.)

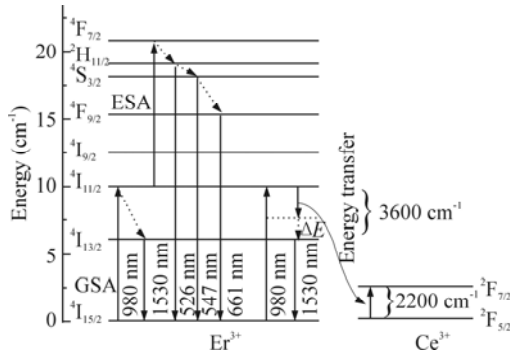

Fig.5 Energy level diagram of Er^{3+} and Ce^{3+} and relevant transitions in the glass sample

The measured 1.53 μm band fluorescence emission spectrum of TBW0 sample, along with the peak fluorescence intensity under the same 980 nm pumping condition, is displayed in Fig.6. It can be found that the full width at half maximum (FWHM) listed in Tab.1 increases from 56 nm to 64 nm with the increase of WO_3 content, which is larger than that of silicate glass (~40 nm), phosphate glass (~37 nm) and germinate glass (~42 nm)[2,16]. The broad 1.53 μm band fluorescence emission can be attributed to the high refractive index (~2.0) of tellurite glass host on the one hand, which promotes the $^4I_{13/2}\rightarrow{}^4I_{15/2}$ transition of Er^{3+}. On the other hand, the presence of multiple structural units ([TeO_4] bipyramidal and [$TeO_{3+\delta}$] trigonal pyramidal units, [BiO_3] pyramidal and [BiO_6] octahedral units[17], [WO_4] tetrahedral and [WO_6] octahedral units[13]) creates a range of various dipole environments which result in further broadening of the fluorescence emission spectra inhomogeneously. Furthermore, the peak fluorescence intensity increases steadily with the increase of WO_3 content. For example, the peak fluorescence intensity of TBW4 glass sample increases by nearly 18% compared with that of the TBW0 glass sample, which can be attributed to the enhanced energy transfer between Er^{3+} and Ce^{3+} ions. As shown in Fig.2, the maximum phonon energy of glass matrix increases from 750 cm^{-1} to 920 cm^{-1}. The larger the phonon energy, the less the phonons needed to bridge the energy mismatch, which exists in the energy transfer process of Er^{3+}:$^4I_{11/2}$+Ce^{3+}:$^2F_{5/2}\rightarrow Er^{3+}$:$^4I_{13/2}$+$Ce^{3+}$:$^2F_{7/2}$. Therefore, the addition of WO_3 into tellurite glass enhances the energy transfer process indeed. As a result, the non-radiative decay rate of Er^{3+}:$^4I_{11/2}\rightarrow{}^4I_{13/2}$ transition is increased further, and the Er^{3+} ions populated at $^4I_{11/2}$ level should get more sparse while those accumulated at $^4I_{13/2}$ level should get more dense, so a much weaker up-conversion emission and a much stronger 1.53 μm band fluorescence can be anticipated, respectively.

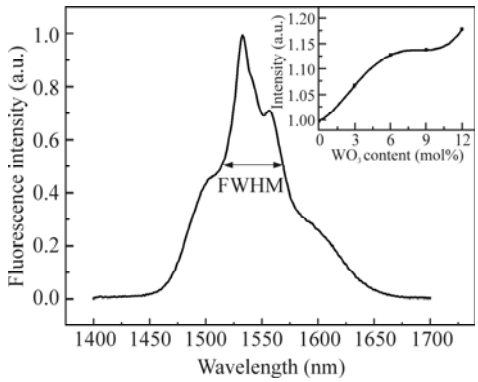

Fig.6 Fluorescence spectrum of TBW0 sample (The inset is emission intensity under pumping of 980 nm.)

FWHM, peak stimulated emission cross-section (σ_e^p) and fluorescence lifetime (τ_m) are the three important spectroscopic parameters for a glass medium applied for the 1.53 μm band EDFA. Amplification characteristics of the EDFA gain medium are mainly described by the gain quality factor and bandwidth quality factor. Bandwidth quality factor is generally measured by the product of σ_e^p and FWHM, and gain quality factor is generally measured by the product of σ_e^p and τ_m [18]. The larger the products, the better the properties of EDFA[6,19].

Tab.1 lists the relevant spectroscopic parameters and amplification quality factors of TBW0–TBW4 samples. The stimulated emission cross-section is obtained from the absorption cross-section of Er^{3+}:$^4I_{15/2}\rightarrow{}^4I_{13/2}$ transition according to the McCumber theory[20]:

$$\sigma_e(\lambda)=\sigma_a(\lambda)\exp[(\varepsilon-h\nu)/kT], \quad (1)$$

where h is the Planck constant, k is the Boltzmann con-

stant, and ε is the net free energy required to excite one Er^{3+} ion from the $^4I_{15/2}$ ground state to $^4I_{13/2}$ excited level at temperature T and can be calculated using the method provided in Ref.[21]. Absorption cross-section is determined from the measured absorption spectra shown in Fig.3 according to the following expression:

$$\sigma_a(\lambda)=\frac{2.303}{NL}OD(\lambda), \quad (2)$$

where $OD(\lambda)$ is the measured optical density, N is the Er^{3+}-doped concentration, and L is the sample thickness.

Tab.1 Stimulated emission cross-sections (σ_e^p), FWHM, fluorescence lifetime (τ_m) at the $^4I_{13/2}$ level, and amplification quality factors of Er^{3+} in tellurite-based glasses

Sample	σ_e^p (10^{-21} cm^2)	*FWHM* (nm)	τ_m (ms)	$\sigma_e^p \times$*FWHM* (10^{-21} cm^2·nm)	$\sigma_e^p \times \tau_m$ (10^{-21} cm^2·ms)
TBW0	6.74	56	2.65	377.44	17.86
TBW1	7.07	61	2.73	431.27	19.30
TBW2	6.94	62	2.74	430.28	19.02
TBW3	7.17	63	2.75	451.71	19.72
TBW4	7.09	64	2.76	453.76	19.57

In Tab.1, it is clearly shown that the bandwidth quality factor developed in this paper is larger than that of silicate glass (22.0×10^{-20} cm^2·nm)[22] and germanate glass (23.9×10^{-20} cm^2·nm)[23], which is attributed to the large stimulated emission cross-section and FWHM, indicating that Er^{3+}/Ce^{3+} co-doped tellurite glass containing WO_3 component is a potential gain medium applied for the 1.53 μm bandbroad EDFA.

In this paper, the WO_3 oxide is introduced into the Er^{3+}/Ce^{3+} codoped TeO_2-Bi_2O_3-TiO_2 glasses. It is found that the prepared tellurite-based glass samples are amorphous in nature, and an appropriate amount of WO_3 can evidently improve the 1.53 μm band fluorescence intensity and meanwhile greatly increase the FWHM and bandwidth quality factors of Er^{3+}. The improvement of 1.53 μm band fluorescence intensity is attributed to the enhanced energy transfer between Er^{3+}/Ce^{3+} ions, while the increase of the FWHM and bandwidth quality factor is due to the inhomogeneous broadening of fluorescence emission. Therefore, as a glass host applied for the 1.53 μm band high gain and broad amplification, an appropriate amount of WO_3 can be selectively introduced into the Er^{3+}/Ce^{3+} co-doped tellurite glass with low phonon energy.

References

[1] M. R. Dousti, M. R. Sahar, S. K. Ghoshal, R. J. Amjad and A. R. Samavati, Journal of Molecular Structure **6**, 1035 (2013).

[2] N. G. Boetti, J. Lousteau, A. Chiasera, M. Ferrari, E. Mura, G. C. Scarpignato, S. Abrate and D. Milanese, Journal of Luminescence **1265**, 132 (2012).

[3] S. Wang, Y. X. Zhou, S. X. Dai, X. S. Wang, X. Shen, Y. Wu and X. C. Xu, Journal of Optoelectronics·Laser **22**, 12 (2011). (in Chinese)

[4] W. Stambouli, H. Elhouichet and M. Ferid, Journal of Molecular Structure **39**, 1028 (2012).

[5] R. S. Chaliha, K. Annapurna, A. Tarafder, V. S. Tiwari, P. K. Gupta and B. Karmakar, Solid State Sciences **1325**, 11 (2009).

[6] I. Jlassi, H. Elhouichet, M. Ferid and C. Barthou, Journal of Luminescence **2394**, 130 (2010).

[7] E. F. Chillcce, I. O. Mazali, O. L. Alves and L. C. Barbosa, Optical Materials **389**, 33 (2011).

[8] J. Yang, L. Zhang, L. Wen, S. Dai, L. Hu and Z. Jiang, Journal of Applied Physics **3020**, 95 (2004).

[9] J. Yang, L. Zhang, L. Wen, S. Dai, L. Hu and Z. Jiang, Chemical Physsics Letters **295**, 384 (2004).

[10] J. Lousteau, N. G. Boetti, A. Chiasera, M. Ferrari, S. Abrate, G. Scarciglia, A. Venturello and D. Milanese, IEEE Photonics Journal **194**, 4 (2012).

[11] Y. G. Choi, K. H. Kim, S. H. Park and J. Heo, Journal Applied Physics **3832**, 88 (2000).

[12] D. Rajesh, Y. C. Ratnakaram and A. Balakrishna, Journal of Alloys and Comounds **22**, 563 (2013).

[13] T. Sekiya, N. Mochida and S. Ogawa, Journal of Non-Crystalline Solids **105**, 176 (1994).

[14] A. Dehelean, S. Rada, A. Popa and E. Culea, Journal of Molecular Structure **203**, 1036 (2013).

[15] J. Qiu, Y. Shimizugawa, Y. Iwabuchi and K. Hirao, Applied Physics Letters **43**, 71 (1997).

[16] S. Jiang, T. Luo and B. C. Hwang, Journal of Non-Crystalline Solids **364**, 263 (2000).

[17] M. Subhadra and P. Kistaiah, Vibrational Spectroscopy **23**, 62 (2012).

[18] J. S. Wang, E. M. Vogel and E. Snitzer, Optical Materials **187**, 3 (1994).

[19] M. Naftaly, S. Shen and A. Jha, Applied Optics **4979**, 39 (2000) .

[20] D. E. Mccumber, Physical Review A **299**, 134 (1964).

[21] W. J. Miniscalo and R. S. Quimby, Optics Letters **258**, 16 (1991).

[22] B. C. Hwang, S. Jiang, T. Luo, K. Seneschal, G. Sorbello, M. Morrell, F. Smektala, S. Honkanen, J. Lucas and N. Peyghambarian, IEEE. Photonics Technology Letters **197**, 13 (2001).

[23] H. Lin, E. Y. B. Pun, S. Q. Man and X. R. Liu, Journal of the Optical Society of America B-Optical Physics **602**, 18 (2001).